

RECOMMENDATIONS FOR RCD GROUND FAULT DETECTOR TRIP THRESHOLDS

Jack Flicker, Kenneth Armijo, and Jay Johnson
 Sandia National Laboratories
 P.O. Box 5800 MS0352
 Albuquerque, NM 87185-0352 USA
 Phone: +1 505-284-9586
 Fax: +1 505-844-3952
 jjohns2@sandia.gov

ABSTRACT: Photovoltaic (PV) ground faults have caused many fires in the U.S. and around the world. Recently, the American PV industry has discovered a blind spot in fuse-based ground fault detection that has spurred a transition to a number of alternatives traditionally used in European markets. This paper investigates the repeatability of one of these methods, residual current detection (RCD), using historical field data from 340 utility-scale inverters in a large 170 MW installation. The distributions of leakage current magnitudes for the inverters is calculated for one year to determine a statistical RCD trip metric that minimizes unwanted tripping but increases the sensitivity of ground fault detection. The RCD current transients were also studied to determine the efficacy using the derivative of RCD current to detect high impedance ground faults

Keywords: photovoltaics, residual current detection, SPICE, ground faults, leakage current

1. INTRODUCTION

PV faults have caused multiple well-documented fires around the world [1, 2]. In cases of ground faults on rooftop systems, the resulting fire can burn down the building and put the occupants' lives at risk. Further, publicity surrounding these fires is changing public perception of solar in harmful ways. In 2013, The U.S. Department of Energy-funded Solar America Board for Codes and Standards (Solar ABCs) steering committee investigated ground faults and the ground fault detection "blind spot" in PV systems with fuse-based ground fault detector/interrupters (GFDIs) [3-5]. The conclusion of the project was American PV systems were vulnerable to faults to the grounded current-carrying conductor (CCC), because the fault current through the fuse may not be sufficient to clear the fuse; and, in the event of a 2nd ground fault, clearing the fuse does not de-energize the fault. As a result, the 2014 U.S. *National Electrical Code® (NEC)* [6] Section 690.5 was updated to explicitly state that ground faults in intentionally grounded conductors must be detected. A number of alternative technologies have been suggested to detect blind spot faults [4] including isolation resistance monitoring (R_{iso}), residual current detection (RCD), and current sense monitoring/relay (CSM/R). In this paper, we focus on RCD technologies and compare the trip thresholds in U.S. and international standards to field leakage measurements to suggest refinements to the standards.

Many RCDs operate by monitoring the differential current flow in the positive and negative CCCs. Any current imbalance between the two CCCs above a preset threshold is assumed to be caused by a ground fault and the RCD trips. In non-AC-isolated systems with transformerless inverters, the fault current is fed from the AC side of the system as well, so the RCD can be installed on the AC side of the inverter.

The range of detectable ground faults from RCD measurements depends on the threshold used to define the presence of a fault. If this trip threshold is too low,

there will be nuisance trip events resulting from module and BOS component leakage currents; but if the threshold is too high, higher impedance ground faults will go undetected. Both RCD and CSM/R methods could register array leakage current as a type of fault, therefore the generalized detection threshold must be set above the maximum leakage current in all unsaulted operating conditions (meteorological, topological, and electrical) in the ground fault detector certification standards, e.g. UL 1741 and IEC 62109-2. In previous work on R_{iso} field measurements and simulations, it was found that inverter insulation-to-ground isolation accounted for the majority of the leakage measurement, rather than the module-to-ground isolation[7]. Similarly, in this report RCD measurements showed inverter-to-ground leakage component accounted for a large portion of the overall system leakage when the PV system is exporting power.

This paper suggests thresholds for RCD devices in a large (170 MW) PV array through a statistical analysis of leakage probability distributions of historical RCD measurements. Based on the large number of measurements, broader suggestions are provided for national and international PV inverter certification standards. However, further analysis is necessary to develop a comprehensive understanding of the range of RCD measurements in unsaulted systems in order to establish robust detection thresholds which balance system performance (uptime), reliability, and safety.

2. RCD STANDARDS

In the U.S., maximum ground fault threshold requirements are included in UL 1741 [8] (Table I). There is an additional UL 1741 certification requirement decision (CRD) for non-isolated [9] PV systems which lower the RCD threshold to 300 mA for inverter nameplate ratings of 30 kVA or smaller. In Canada, CSAI07.1 [10] is in agreement with the UL 1741 CRD. Elsewhere, standard maximum RCD thresholds are determined by IEC62109-2 [11], which states that

thresholds should be set at 300 mA for inverter capacities of 30 kVA or less. For inverters larger than 30 kVA in capacity, maximum RCD thresholds are 10 mA per kVA. The UL CRD and IEC standard also require the RCD to trip if there are significant step changes in the RCD measurement.

Table I: Summary of RCD Thresholds in U.S. and International Standards.

Standard	RCD	
UL 1741, Ed. 2 [8]	System kW	mA
	0 - 25	≤ 1000
	25 - 50	≤ 2000
	50 - 100	≤ 3000
	100 - 250	≤ 4000
	>250	≤ 5000
UL 1741 CRD 26-Apr-2010 [12] ($S_{max} \leq 30$ kVA)	mA	Trip time (s)
	300 continuous	0.30
	30 step	0.30
	60 step	0.15
	150 step	0.04
	mA	Trip time (s)
IEC 62109-2, Ed. 1 [13]	≤ 30 kVA = 300 mA RMS (continuous)	0.30
	>30 kVA = 10 mA RMS per kVA (continuous)	
	30 (step)	0.30
	60 (step)	0.15
	150 (step)	0.04
	S_{max} is the maximum rated inverter output apparent power in kVA, where kVA values are the rated continuous output power of the Equipment Under Test. RMS is root mean square.	

3., HISTORICAL LEAKAGE DATA

3.1 Utility-Scale Systems

The system leakage values of 340 500 kW co-located inverters in a desert environment were measured at one-minute intervals for over a year (1 January 2013 to 3 August 2014) using RCDs. In compliance with UL 1741, each inverter has a GFDI fuse rated at 5 A to protect against ground faults (Table I). This conservative threshold was chosen to maximize the detection of ground faults while eliminating unwanted tripping events due to electromagnetic interference (EMI), module/inverter leakage, and meteorological events (i.e. lightning).

Figure 1 shows leakage data from a single inverter (data is typical for all the 500 kW inverters) at one-minute intervals over the course of a year (blue trace) as well as the 24-hour average of the leakage current (black dots) and the ambient temperature (red trace). As can be seen from the data, at no point during the year did the leakage current exceed 2.57 A. Excluding transient spikes in leakage current due to inverter start-up or shutdown when the DC contactor was closed, the maximum daily inverter leakage is approximately 1.1 A with a minimum daily inverter leakage of approximately 0.38 A at night. This minimum is influenced both by the RCD detection threshold and nighttime inverter behavior. At night, the inverter isolates from the AC and DC-side and relies on a 3 A GFDI fuse on the ground bound for

ground fault detection rather than the RCD. Therefore, the actual minimum leakage current is most likely lower than the recorded nighttime RCD current of 0.38 A. These historical RCD values indicate that there is significant overhead in the 5 A GFDI rating and the GFDI fusing or RCD trip threshold could be reduced to 3 A or less.

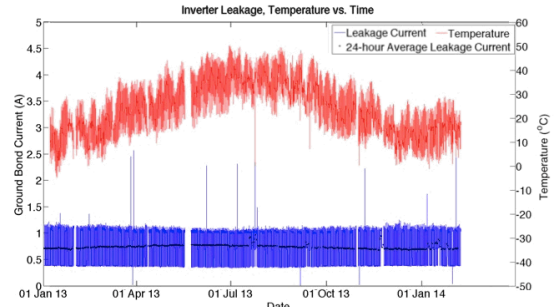


Figure 1: Typical leakage current data from a 500 kW inverter taken at one-minute intervals (blue trace) and averaged over a 24-hour window (black dots). The ambient temperature is also shown over one-minute intervals (red trace).

Figure 2 shows a weeklong subset of the data from seven inverters. The inverter-to-inverter variation in leakage current is nearly identical during the turn-on/turn-off periods. During the turn-on/turn-off period, the RCD current temporarily stagnates at a value of approximately 0.7 A. This shoulder lasts approximately 30 minutes while there is sufficient voltage (~175 V) to turn on the RCD and power electronics components in the inverter, but not enough photocurrent to initiate the inversion process. Once the available array current increases to a sufficient value (~700 V), the inverter begins MPPT and the leakage current steps to around 1.1 A. Throughout the day, the inverter-to-inverter variation in the leakage current is around 200 mA. The RCD morning shoulder also exists during inverter turn-off as the bus voltage decreases at the end of the day.

During the week shown, one of the CTs attached to Inverter 7 measured a current spike—also seen in Figure 1. These spikes are not correlated between inverters (even those in geographical and electrical proximity to each other) and seem to occur at random, although they are always associated with inverter turn-on or turn-off. The inset of Figure 2 shows a detailed view of the current spike. The turn-on spike lasts from 07:26 to 07:34 with a linear increase in current leakage from a “shoulder” turn-on leakage of 0.685 A to a maximum leakage of 1.676 A. After the maximum, the leakage current quickly decreases to a steady on-state leakage current value of 1.058 A. It is believed the DC contactor operation at the beginning and end of the day is causing the spikes in the current as the array capacitance is discharged. This only appears for some mornings/afternoons because it is a quick transient that is not always caught by the data acquisition system. The multi-minute spike in the inset is most likely the result of the data historian compression and only a single measurement is recorded during the current impulse. Since this is a quick transient with an extremely small number of readings, it is unknown if these spikes will trip the RCD protection circuit if the threshold is set below the magnitude of the spike. Single, isolated measurements in the data above the 5 A trip

threshold do not result in inverter shutdown, so it is unlikely that these transients will cause the RCD to detect the presence of a fault and initiate inverter shut-down. Notably, GFDI fuses intrinsically have resistance to transient events because they are thermally actuated; therefore, as ground fault detection in the U.S. is converted to electrical measurements, it is important to engineer in trip logic robustness with respect to transient currents.

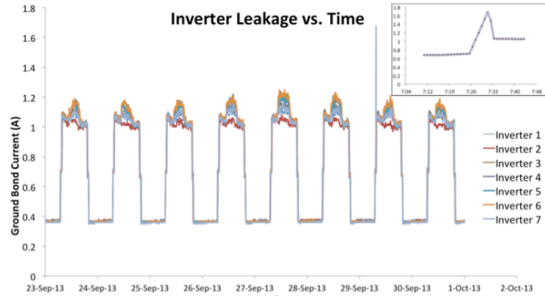


Figure 2: Leakage current data over a week for the seven inverters monitored. A turn-on spike in the leakage current can be seen from Inverter 7 on 29 September 2013 with a close-up view of the spike event shown in the inset.

3.2 Leakage Current and Voltage

The inverter leakage has a relatively constant maximum of approximately 0.76 A for all bus voltages between 100 and 600 V, shown in Figure 3. There is a discrete change in inverter leakage for bus voltages above 600 V, at which point the maximum leakage value is reached at 1.1 A. This abrupt increase in leakage current occurs as the inverter begins to export power from the array to the grid. During high irradiance days, the inverters operate in power clipping (PC) mode. In PC mode, the DC power is larger than the maximum inverter nameplate power, so the inverter moves to an operating point with voltages greater than V_{mp} . This acts to decrease the DC input power to the inverter kVA rating while also minimizing I^2R losses. PC mode is necessary in this system because the array was designed with a DC:AC power ratio above 1. The leakage measurements associated with PC mode are plotted in red in Figure 3. From the data collected, there is no increase in measured RCD leakage current in PC mode, regardless of the increased operational voltage of the array.

In order to more clearly see how measured RCD current varies as a function of array voltage, the inset of Figure 3 shows the RCD current as a function of array voltage for a single inverter for one day (12 July 2013 23:59-13 July 2013 23:59). At night, the inverter is disconnected from the array, so the RCD records the nighttime baseline of ~ 0.35 A. When the sun rises, the array voltage increases, but the DC power is too low for the inverter to turn on (line A in inset). Once the array voltage reaches 175 V, the electronics in the inverter turn on and the measured leakage value increases (B). The DC power is still too low for the inverter to begin MPPT, so the RCD current is a constant value (C) that corresponds to the turn-on shoulder. Once the array voltage increases to 700 V, the inverter can connect to the array (D) and begin MPPT (E). The RCD current ranges between 1 and 1.1 A for the entire day of operation. As the sun sets and the array voltage falls below 600 V, the

inverter disconnects from the array (F). The RCD current stays at a constant value corresponding to the turn-off shoulder (G) until the array voltage decreases below 200

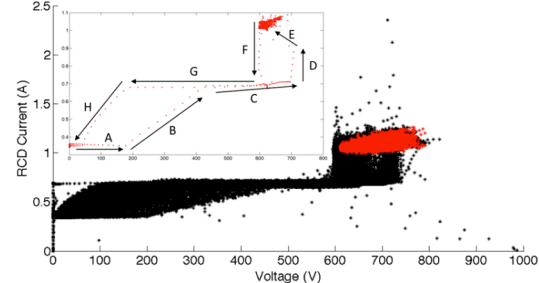


Figure 3: RCD current as a function of bus voltage for an inverter measured over 1 year. PC mode (plotted in red) does not yield a noticeable increase in measured leakage. The inset shows a subset of the data for single day (14 July 2013-15 July 2013). The arrows correspond to the time evolution of the leakage showing operation at nighttime (A), prior to turn-on shoulder (B), RCD turn-on shoulder (C), inverter turn-on (D), MPPT (E), inverter turn-off (F), RCD turn-off shoulder (G), and post turn-off shoulder (H).

V and there is insufficient voltage present to keep the ancillary inverter functions operating, causing the RCD current to fall (H) back to the nighttime baseline value.

As shown in Figure 4, the average 24-hr leakage current is correlated with the 24-hr average of the bus voltage. In the winter, the maximum daily leakage values are larger because the array has a higher operating voltage (due to lower temperatures). However, both the average leakage and average voltages values are smaller due to fewer daylight operational hours. In the summer, there are more daylight hours, so both the average leakage and the average bus voltage increases, while the maximum daily leakage value decreases due to the higher ambient temperatures. The spikes in the average voltage occur during days when the inverter was not operating and the array was at V_{oc} . These also correspond to higher average leakage currents, indicating the bus voltage is a major driver of leakage current through the modules and inverter.

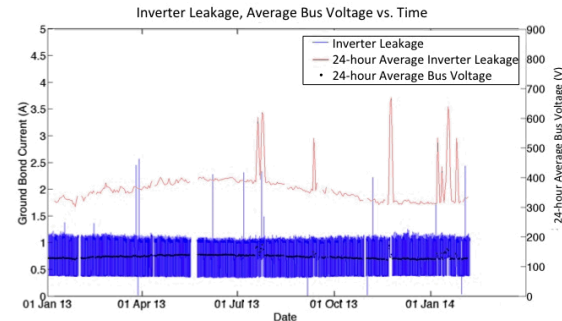


Figure 4: Typical leakage current data from a 500 kW inverter taken at one-minute intervals (blue trace), leakage current averaged over a 24-hour window (black dots), and 1-day bus voltage average (red trace).

3.3 Statistical Analysis of the Leakage Current

When describing proper RCD thresholds for ground fault protection, there are three statistical parameters that are of great importance: the average functional leakage of

a group of inverters, their standard deviation, and the maximum measured leakage values. The leakage average and standard deviation of a group of inverters is useful for advanced fault detection techniques such as decision tree or outlier detection [14-16]. The maximum leakage values are used for simple thresholding to determine the presence of a fault.

(top) shows the raw cumulative distribution functions (CDFs) of all 340 RCDs for one year. Each CDF has a similar multi-tiered shape with a large increase in frequency of measurements at ~ 0.35 A corresponding to the nighttime baseline of the inverters. A second increase to 50% frequency occurs at ~ 0.7 A, corresponding to the turn-on/turn-off shoulder leakage. Finally, about 50% of the leakage frequency occurs in the 0.8 to 1.2 A range, corresponding to daytime leakage values. For a given CDF curve, a shift to the right indicates higher leakages in the inverter possibly due to an incorrect baseline value or a high impedance ground fault. A shift up and down typically indicate data drop-outs where the RCD monitor repeats certain values for extended periods of time. Data dropouts and incorrect baseline values contribute to the spread in the CDFs of the inverters. If these effects are corrected (which can be done via simple, on-board programming), such as baselining the inverter leakage each night when the inverter is disconnected and eliminating repeated data due to drop-outs, the CDFs of all 340 inverters are surprisingly tightly distributed (Figure 5 bottom) **Error!**

Reference source not found. When inverters are properly baselined and data drop-outs are accounted for, all but five of the 340 inverters (colored in blue in Figure 5 bottom) lie within a range of 1.14–1.51 A at 99.99% frequency. The five inverters that act as outliers (CDFs are different colors) have either higher or lower leakage values than normal. The RCD values over a six-day period of these outlier inverters along with a “typical inverter” (blue) are shown in the inset.

The inverters corresponding to the magenta, green, and black curves show higher measured leakage values during the day while the red curve corresponds to a lower measured leakage value. It should be noted that, although the baseline for each inverter is the same, the turn-off/turn-on shoulder values scale with the daytime leakage of the inverter, indicating that the increased or decreased RCD current may be due to a proportionality (gain) problem in the RCD rather than an actual increase of leakage in the inverter.

The 4σ and 6σ confidence bands of the average CDF of all the inverters (both “normal” and the five outlier inverters) is shown as dashed black lines in (Figure 5 bottom). Note that these curves represent RCD values that are exceeding rare given the data population: $\Pr(x \geq \mu+4\sigma) = 0.00317\%$ and $\Pr(x \geq \mu+6\sigma) = 9.87 \cdot 10^{-8}\%$. These statistical metrics can be used to establish thresholding rules based on the requirements of the inverter manufacturer, O&M company, plant owner, or standards-making panel. For example, there is a 4σ confidence that 99.999% of measured leakage values are below 3.1994 A and a 6σ confidence that 99.999% of the RCD values are below 3.8616 A (

Table II). A set point of 5 A (as currently mandated by UL 1741) corresponds to an eight-nines confidence of the 4σ confidence band.

For simple thresholding practices, the distribution of leakages for an inverter is of little importance as only the instantaneous leakage value is used to detect the presence

of a fault. Therefore, the maximum leakage values of

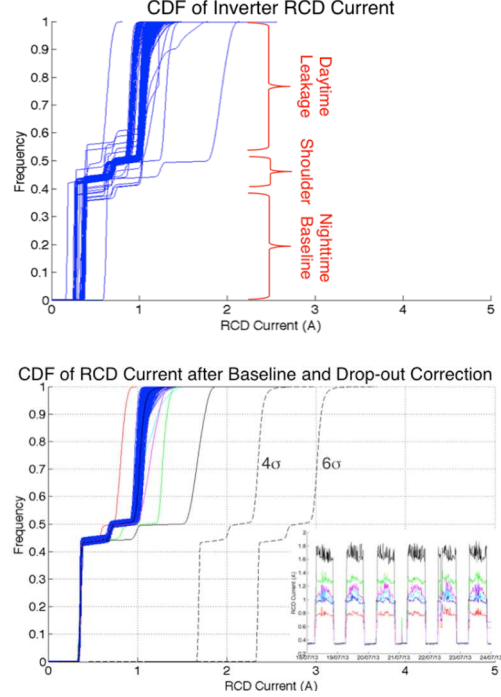


Figure 5: (top) Raw CDFs of inverter leakage for 340 inverters. The CDFs have three distinct sections due to nighttime baseline leakage at ~ 0.35 A, the turn-on/turn-off shoulder at ~ 0.7 A, and the daytime leakage at ~ 1 A. (bottom) CDFs corrected for baseline and data dropouts. Most of the CDFs are clustered together with a few outlier inverters with higher or lower leakages (shown in inset). Assuming a normal distribution, the $+4\sigma$ and $+6\sigma$ limits of the average CDF are shown as black dashed lines.

monitored inverters are most important. **Error!**

Reference source not found. Figure 7 shows a series of histograms of the measured leakage values of all 340 inverters. At the global level (Figure 6 top), the leakage values cluster into three groups corresponding to the nighttime baseline (~ 0.32 – 0.38 A), the turn-on/turn-off shoulder (~ 0.64 – 0.72 A), and the daytime leakage (~ 0.92 – 1.39 A).

Table II: High frequency values of the CDFs for the average of all inverters as well as the 4σ and 6σ confidence bands.

Frequency (%)	Average	4σ	6σ
99	1.1825	2.5067	3.1688
99.9	1.6437	2.9679	3.6300
99.99	1.8028	3.1270	3.7892
99.999	1.8752	3.1994	3.8616
99.9999	2.4891	3.8133	4.4754
99.99999	2.8759	4.2001	4.8623
99.999999	3.6827	5.0069	5.6690

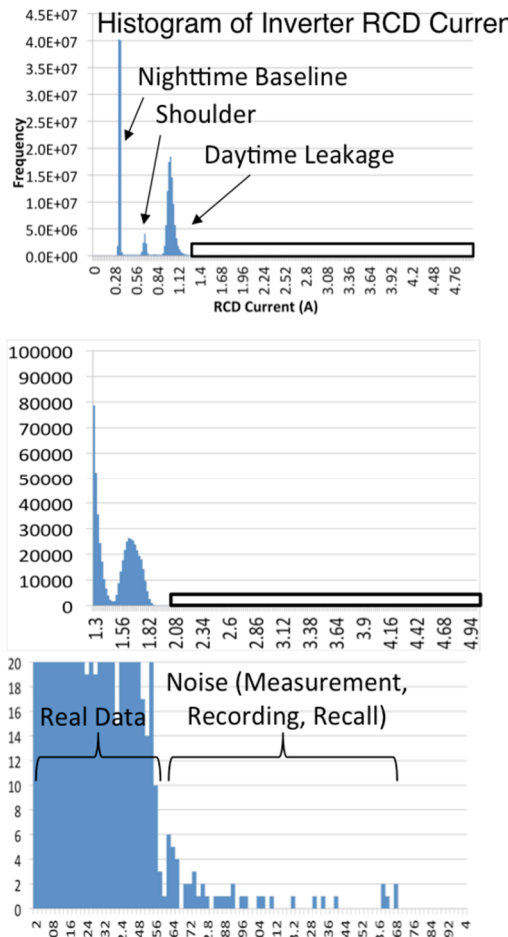


Figure 6: Histogram of baseline and dropout corrected leakage values for 340 inverters. The majority of points are contained in three groups below 2 A (nighttime baseline, turn-on/turn-off shoulder, and daytime leakage). Between 2.5 and 3.75 A, a small number of points were measured, although many of these single measured points can most likely be attributed to noise in RCD measurement, recording, or recall.

At higher RCD currents, there is another distribution of values from 1.50-1.82 A (Figure 6 middle) most likely corresponding to the capacitive discharge spikes that occur when the inverter first connects to the array, as seen in Figure 2 (inset). At even larger currents, there are a small number of points (<10) in the 2.5-4.0 A range (**Error! Reference source not found.** bottom). Due to the large number of data points collected and the compression algorithm of the server, it is assumed that these high current, low frequency data points are noise in the measurement, recording or transient events. This is corroborated by the fact that a single leakage value of ~8 A was recorded for one inverter. This single measured RCD current above the trip threshold of 5 A did not cause the inverter to trip due to a ground fault. Therefore, single, high current leakage values are most likely measurement errors that can be safely discounted when determining appropriate trip points for the RCD monitor. As can be determined from the large-scale, long-term data presented here, trip points for the inverter could

easily be lowered from 5 A to 3 A with no observable increase in nuisance tripping events.

3.4 Derivative of RCD current

In addition to mandating the maximum instantaneous leakage for a system, UL and IEC standards also mandate the maximum point-to-point variation in the leakage. In order to analyze this set point, the derivative of the RCD current was analyzed as a function of window averaging. Figure 7 (top) shows the derivative of the RCD measurement of a single inverter over a single day as a function of uniform averaging of 1 (magenta), 2 (cyan), 4 (red), 8 (green), 16 (blue), or 32 (black) minutes.

For the typical day, as the inverter connected to the array and the leakage current increased, there are two positive spikes to ~0.035 A/min corresponding to the RCD current increases before and after the turn-on shoulder. During normal daytime operation, the derivative varies between ± 0.07 A/min (since a negative derivative indicates a decrease in the RCD current, it is never used to indicate the presence of a fault). Two negative spikes occur as the leakage current decreases when the inverter disconnects from the array.

The RCD measurement averaging acts as a smoothing function, eliminating sharp changes in the derivative. Such a windowing function using past measurements could be used to eliminate nuisance tripping due to transients or noisy measurements, however such filtering comes at the expense of response time, which may not be acceptable due to safety concerns. As shown in the trip times in Table I, response times for transient events are less than 1 second, so the sampling rate of the RCD would need to be in the 10s to 100s of Hz to perform effective averaging.

Figure 7 (bottom) shows the histogram of the derivative of the RCD current for window averaging of 1 (magenta), 2 (cyan), 4 (red), and 8 (green) minutes. The derivative values are an extremely tight distribution and only the extremes of the distribution tails (<15 points) are shown.

For no window averaging, the value of the derivative is mostly between 0 and 0.37 A/min with the frequency of values decreasing rapidly to 1 A/min with single digit frequencies for RCD currents larger than 1 A/min. Due to a single measurement point of the RCD current (most likely due to noise as discussed above), the maximum value registered for this inverter was 7.88 A/min. For an averaging window of two points, the distribution tightens by a factor of two and the maximum derivative reading halves to 3.94 A/min. As the window increases, the distribution continues to tighten.

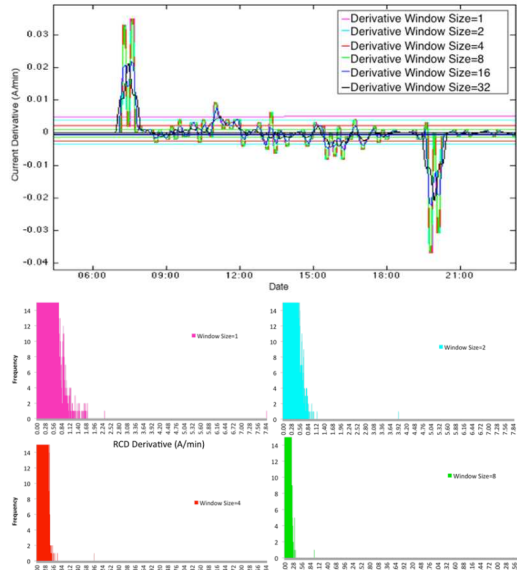


Figure 7: (top) The RCD current derivative of an inverter for a typical day. The two positive spikes at the beginning of the day correspond to RCD current increases before and after the turn-on shoulder. During operation the derivative varies between ± 0.035 . At the end of the day, two negative spikes occur as the RCD current decreases before and after the turn-off shoulder. (bottom) histogram of RCD current derivative as a function of averaging window. The distribution tightens as the function is smoothed due to an increase in the window.

4. CONCLUSIONS

PV fires due to ground faults are a significant danger to the future of PV plant operations. In the US, Solar ABCs has identified gaps in traditional (i.e. fuse-based) ground fault detection techniques and recommended moving to other methods (i.e. R_{iso} and RCD monitoring). In order to improve and harmonize IEC and UL standards, the RCD leakage values of 340 co-located inverters has been analyzed for over a year. Based on this data, the static RCD requirements in IEC 62109-2 and UL 1741 CRDs were found to be overly conservative.

For these inverter models at this location, the RCD thresholds could be reduced to improve high impedance ground fault sensitivity without an increase in unwanted tripping. For an average inverter in this array, the RCD trip point could be lowered from 5 A to as low as 2.5 A with six 9's confidence that any measured RCD value would be lower than the setpoint. Statistically, this would correspond to 0.5 trips/year/inverter if single, raw RCD measurement points are considered. In practice, this number would be drastically reduced through the proper use of data windowing, averaging, or other simple data analysis techniques.

The transient (i.e. sudden increase) values were not fully analyzed and compared to existing standards because the temporal data fidelity did not provide sufficient resolution for a true comparison⁵. The IEC standard sudden change bounds resulted in no faults from the data observed over the monitoring period even with large single-point increased in RCD current. Further work must be done to compare these transient trip settings with high-fidelity RCD data to make similar recommendations for trip points.

5. ACKNOWLEDGEMENTS

This work was funded by the DOE Office of Energy Efficiency and Renewable Energy. Sandia National Laboratories is a multi-program laboratory managed and operated by Sandia Corporation, a wholly owned subsidiary of Lockheed Martin Corporation, for the U.S. Department of Energy's National Nuclear Security Administration under contract DE-AC04-94AL85000.

6. REFERENCES

- [1] B. Brooks, "The Ground-Fault Protection Blind Spot: Safety Concern for Larger PV Systems in the U.S.," Solar American Board for Codes and Standards, January 2012.
- [2] H. Laukamp, "Statistical Failure Analysis of German PV Installations," *PV Brandsicherheit Workshop*, Köln, Germany, 26 Jan. 2012 (in German).
- [3] J. Flicker and J. Johnson, "Photovoltaic Ground Fault and Blind Spot Electrical Simulations," Sandia National Laboratories, 2013.
- [4] G. Ball, B. Brooks, J. Flicker, J. Johnson, A. Rosenthal, J. C. Wiles, and L. Sherwood, "Inverter ground-fault detection 'blind spot' and mitigation methods," Solar American Board for Codes and Standards, June 2013.
- [5] J. Flicker and J. Johnson, "Analysis of Fuses for 'Blind Spot' Ground Fault Detection in Photovoltaic Systems," Solar American Board for Codes and Standards, Jul 2013. Available: http://solarabcs.net/about/publications/reports/blinds_pot/pdfs/analysis_of_fuses-June-2013.pdf
- [6] National Fire Protection Association, "National Electrical Code, 2014 Edition, NFPA70." Quincy, MA.
- [7] J. Flicker, J. Johnson, M. Albers, and G. Ball, "Recommendations for CSM and Riso Ground Fault Detector Trip Thresholds," *2014 IEEE Photovoltaic Specialists Conference*, Denver, CO, 2014.
- [8] Underwriters Laboratories 1741 Ed. 2, "Inverters, Converters, Controllers and Interconnection System Equipment for Use With Distributed Energy Resources," 2010.
- [9] Underwriters Laboratories 1741 Ed. 2, "Non-isolated EPS Interactive PV Inverters Rated Less than 30 kVA," 2010.
- [10] CSA International C22.2 No. 107.1, "General Use Power Supplies." Toronto, ON, 2011.
- [11] International Electrotechnical Commission IEC62109-2 ed 1.0, "Safety of power converters for use in photovoltaic power systems - Part 2: Particular requirements for inverters ". Geneva, Switzerland, 2011.

- [12] Underwriters Laboratories 1741, "Certification Requirement Decision, Non-Isolated EPS Interactive PV Inverters Rated Less Than 30kVA," 26-April-2010.
- [13] International Electrotechnical Commission 62109-2 Ed. 1.0, "Safety of power converters for use in photovoltaic power systems - Part 2: Particular requirements for inverters." Geneva, 2011.
- [14] Y. Zhao, L. Yang, B. Lehman, J. F. de Palma, J. Mosesian, and R. Lyons, "Decision tree-based fault detection and classification in solar photovoltaic arrays," Applied Power Electronics Conference and Exposition (APEC), 2012 Twenty-Seventh Annual IEEE, 2012.
- [15] Y. Zhao, B. Lehman, R. Ball, J. Mosesian, and J.-F. de Palma, "Outlier detection rules for fault detection in solar photovoltaic arrays," Applied Power Electronics Conference and Exposition (APEC), 2013 Twenty-Eighth Annual IEEE, 2013.
- [16] D. Riley and J. Johnson, "Photovoltaic prognostics and health management using learning algorithms," Photovoltaic Specialists Conference (PVSC), 2012 38th IEEE, 2012.